Sensors and Materials, Vol. 36, No. 11 (2024) 4965–4974
MYU Tokyo

S & M 3843

Design of 5G Millimeter-wave Filtering Antenna with Γ-shaped Slot Radiators Coupled to Substrate Integrated Waveguide Cavity

Haitao Xing,* Jianmei Huang, and Zhonghua Ma

School of Marine Information Engineering, Jimei University,
No. 183, Yinjiang Road, Jimei District, Xiamen, Fujian 361021, China

(Received June 11, 2024; accepted October 17, 2024)

Keywords: antennas, microstrip filters, millimeter wave, 5G mobile communication

In this article, we describe the design of the substrate integrated waveguide (SIW) millimeter-wave filtering antenna for 5G communication. It comprises a Γ-shaped slot antenna integrated into a SIW resonant cavity and a bandpass filter (BPF) based on a SIW coupled resonant cavity, which are directly cascaded to form a filtering antenna. The BPF is made up of six resonant cavities, with the opening size between the fourth-order resonant cavities adjusted to achieve magnetic coupling between them. This results in the desired bandpass characteristics. The antenna's radiation is generated by the Γ-shaped slot structure. To verify the proposed structure and design concept, the filtering antenna was manufactured and measured. The simulated and measured results showed good consistency. The −10 dB impedance fraction bandwidth of the antenna is 2% (25.2–25.7 GHz), with a flat gain of 5.9 dBi within the operating range. The proposed filtering antenna has low loss, simple structure, and low cost, and it is easy to integrate with other electromagnetic sensor systems. It is well suited for the 5G millimeter-wave band and is anticipated to remain compatible with future generations of mobile communication systems.

1. Introduction

To cater to the demands of 5G technology, such as high-speed, high-capacity, and low-latency data transmission, mobile communication technology has expanded into the millimeter-wave frequency band.(1) In the 5G millimeter-wave front-end, filters are crucial for suppressing band interference and selecting useful signals. However, conventional filters often suffer from high insertion losses owing to their low quality factors, whereas filters with high-quality factors are challenging to integrate into 5G millimeter-wave systems owing to their large size.(2) To address this challenge, an effective approach is to merge the filtering response with the antenna, forming what is known as a filtering antenna. This integration simplifies the design of millimeter-wave RF front-end filters to some extent.

The appropriate integration of antennas and filters is an effective method to reduce the cost and functional block size of electromagnetic sensor systems. The filtering antenna combines the functionalities of both the antenna and the filter, with design methods primarily employing the

*Corresponding author: e-mail: xht2005@jmu.edu.cn
https://doi.org/10.18494/SAM5170

ISSN 0914-4935

direct cascade method and the equivalent substitution method.[3–7] The design of the direct cascade method is simple, and the filtering and radiation characteristics will not be affected. The disadvantage is that the insertion loss cannot be effectively reduced. The equivalent substitution method can reduce insertion loss and result in a smaller size, but the directional pattern and filtering characteristics are prone to distortion.

Le Nadan *et al*. first introduced the concept of using slot line dipole antennas for designing integrated filters and antennas, where the antenna functions as both the radiator and ultimate resonator of the bandpass filter (BPF).[8] Subsequently, numerous filtering antennas have been continually developed, but most of these filtering antennas operated on SUB-6G.[9–11] The utilization of substrate integrated waveguide (SIW) filters has emerged as a prominent area of research owing to their benefits such as high quality factor, substantial power handling capacity, cost-effectiveness, minimal radiation losses, and seamless integration with planar circuits. In recent years, several SIW-based millimeter-wave filtering antennas have been introduced. Chu *et al*. proposed a 3D filtering antenna with high selectivity and low cross polarization.[12] The back-fed double-slot antenna is both the radiator and final resonator of the BPF. Its center frequency is 31.5 GHz, fractional bandwidth (FBW) is 1.56%, and maximum measurement gain is 6.79 dBi.[12] Fan *et al*. introduced a linearly polarized quarter mode SIW (QMSIW) filtering antenna that eliminates the need for additional filter circuits.[13] The antenna's operating frequency is 24.6–29.6 GHz, the −10 dB impedance FBW is 18.45%, and the average gain is 5.7 dBi.[13] Lu *et al*. developed a dual-polarization filtering antenna that can generate a fourth-order filtering antenna response.[14] The filtering antenna covers 23.2–29.5 GHz, with the FBW of 19.5% and the average gain of 4.5 dBi.[14] Although the above designs demonstrate excellent filtering antenna characteristics, they require a multilayer structure, which is complex and cannot be well integrated with circuit boards.

In this study, we designed a filtering antenna operating at 25.2–25.7 GHz using the SIW single-layer structure. The bandpass characteristics of SIW are achieved by adjusting the size of the coupling opening between the adjacent cavities. The slot antenna serves as a radiator and cascades with the SIW filter. To verify the proposed scheme, SIW BPFs and SIW filtering antennas were manufactured and measured. The consistency between the measurement results and the simulation structure is good. Compared with other SIW filtering antennas of the same type, this design offers a simple structure, low loss, and high gain, and it exhibits good performance competitiveness.

2. Theory of SIW

SIW, initially introduced by the Canadian scholar Professor Ke Wu, consists of dielectric medium, upper, and lower metal layers, and two sets of metallic via holes.[15] The metalized through-hole wall forms a magnetic wall, which connects the upper and lower metal surfaces of the substrate to form an electrical wall. The basic structure of SIW is shown in Fig. 1. The short-side width is W_{SIW}, the long-side width is L_{SIW}, the through-hole diameter is d, the through-hole spacing (center distance) is s, and the thickness of the dielectric substrate is h.

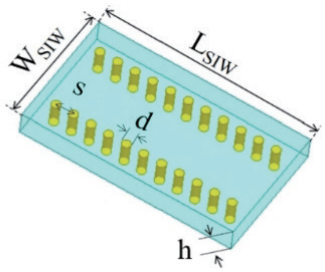

Fig. 1. (Color online) SIW structure schematic.

Owing to the presence of gaps between metalized through-holes, there are certain requirements for the size of these gaps in an actual design to prevent electromagnetic wave leakage. If the diameter d of the through-hole and the gap s between adjacent through-holes satisfy "(1)" to "(3)," electromagnetic leakage can generally be ignored.[16]

$$d < 0.2\lambda_g \tag{1}$$

$$d < 0.2W_{SIW} \tag{2}$$

$$s < 2d \tag{3}$$

The calculation formula for the resonant frequency of the SIW resonant cavity is given as[17]

$$f_{TE_{m0n}} = \frac{c}{2\sqrt{\mu_r \varepsilon_r}} \sqrt{\left(\frac{m}{W_{eff}}\right)^2 + \left(\frac{n}{L_{eff}}\right)^2} \tag{4}$$

where c is the speed of light, equal to 3×10^{11} mm/s, μ_r is the relative magnetic permeability, ε_r is the relative dielectric constant, and W_{eff} and L_{eff} are the equivalent width and length of the SIW, respectively. The fundamental mode of the SIW is the TE_{101} mode, corresponding to TE_{m0n}, where m and n represent the number of modes along the x- and z-directions, respectively. Considering the effect of through-holes, the exact calculation formulas for W_{eff} and L_{eff} are as follows.[18]

$$W_{eff} = W_{SIW} - \frac{d^2}{0.95s} + \frac{0.1d^2}{W_{SIW}} \tag{5}$$

$$L_{eff} = L_{SIW} - \frac{d^2}{0.95s} + \frac{0.1d^2}{L_{SIW}} \tag{6}$$

When the values of s/d and W_{eff} are determined, the radiation loss of the SIW structure and the value of d/W_{SIW} form a positive feedback loop, where the radiation loss of the SIW structure decreases as d/W_{SIW} decreases. The radiation loss of the signal in the SIW resonant cavity decreases as the diameter of the metal via d increases.

3. Filtering Antenna Design

The simplest design method for filtering antennas is to directly cascade the filter and antenna to select the desired signal and suppress the interference outside the operating frequency band. This method is straightforward and convenient, requiring only the matching of port impedances between the filter and the antenna. It allows for the separate design and adjustment of both components. Generally, a BPF with a narrower operating frequency range than the antenna is cascaded with the antenna. In this study, we adopted the SIW structure to design the BPF, and on the basis of this, cascaded the Γ-shaped slot SIW antenna to the output of the filter to achieve the antenna bandpass filtering response.

3.1 SIW BPF structure

To extract the coupling coefficients and external quality factors of the filter, it is first necessary to perform matrix synthesis to obtain the coupling matrix. The normalized coupling matrix obtained using a fourth-order filter is as follows.

$$m = \begin{bmatrix} 0 & 0.9146 & 0 & 0 & 0 & 0 \\ 0.9146 & 0 & 0.8021 & 0 & 0 & 0 \\ 0 & 0.8021 & 0 & 0.6426 & 0 & 0 \\ 0 & 0 & 0.6426 & 0 & 0.8021 & 0 \\ 0 & 0 & 0 & 0.8021 & 0 & 0.9146 \\ 0 & 0 & 0 & 0 & 0.9146 & 0 \end{bmatrix} \tag{7}$$

On the basis of the normalized coupling matrix m and the FBW of the filter, the coupling coefficient k and external quality factor Q_e of the BPF can be determined as follows.[19]

$$k = FBW \cdot m_{ij} \tag{8}$$

$$Q_e = \frac{1}{FBW \cdot m_{ij}} \tag{9}$$

Figure 2 shows the proposed SIW millimeter-wave BPF structure. The substrate material is a Rogers 5880 microwave dielectric plate, with a relative permittivity of 2.2, a loss tangent of 0.0009, and a dielectric thickness of 0.8 mm. The area of the filter is 27 × 19.5 mm^2. Using the

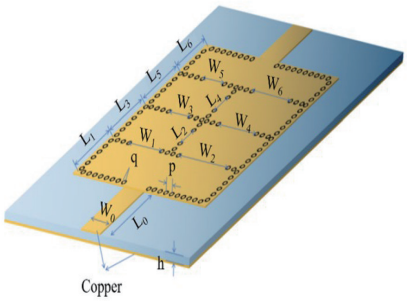

Fig. 2. (Color online) Structure of proposed SIW BPF.

HFSS electromagnetic simulation software, we established the structural model of the SIW fourth-order coupled BPF, where the input and output terminals adopt a microstrip line direct-transition-type conversion structure. Openings are created in the middle of the metallic via walls between adjacent resonant cavities to achieve coupling. The coupling strength is closely related to the length of the coupling opening. By optimizing the structural parameters of SIW and changing the size of the resonant cavity, the optimal structural parameters shown in Table 1 were obtained.

Figure 3 shows the frequency response curve of the SIW BPF obtained through simulation. According to Fig. 3, the operating frequency of the BPF ranges from 24.9 to 25.9 GHz, with the 3 dB passband width of 1000 MHz and the relative bandwidth of 4%. The insertion loss at the center frequency of 25.4 GHz is 0.38 dB, and the reflection within the passband is less than −20 dB.

3.2 Filtering antenna design

The Γ-shaped slot SIW antenna is cascaded at the output end of the filter, and the size of the last stage resonant cavity of the filter is adjusted to match well with the antenna. The designed filtering antenna structure is shown in Fig. 4. To further verify the feasibility of this design method, we manufactured and measured the designed antenna with the area of 32 × 19.5 mm^2 and the thickness of 0.8 mm, as shown in Fig. 5.

Figures 6 and 7 show the simulated and measured reflection coefficients and gains of the filtering antenna, respectively. The impedance bandwidth of the antenna element with a reflection coefficient less than −10 dB measured in the 5G millimeter-wave frequency band (25.2–25.7 GHz) is 2%. The measured reflection within the passband is about 10 dB larger than the simulated reflection, mainly owing to transmission losses caused by manufacturing tolerances. The attenuation of antenna gain outside the passband at 24 and 26.5 GHz exceeds 18 dB, and the simulated attenuation at the upper stopband is greater than the measured value. Particularly at 26.5 GHz, the measured suppression level is about 13 dB lower than the simulated value, which may be due to significant changes in the electromagnetic characteristics of the material as the frequency increases. Similarly to the above filter tests, the measured bandwidth of the filtering antenna is slightly larger than the simulated value. The slight difference between

Table 1
Final parameters of proposed filter (unit: mm).

W_0	W_1	W_2	W_3	W_4	W_5	W_6	p
2.5	4.2	4	4.2	4.2	5	5.2	0.85
L_0	L_1	L_2	L_3	L_4	L_5	L_6	q
3.6	4	2	5	2	5	5	0.48

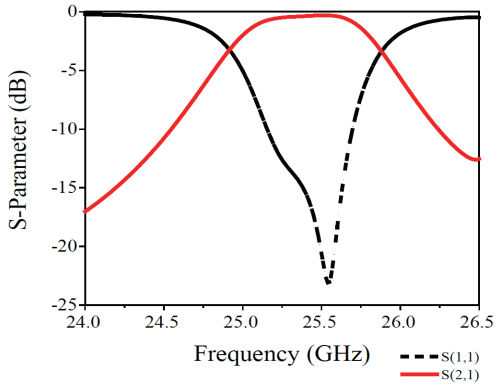

Fig. 3. (Color online) Simulated S-parameter curves of SIW BPF.

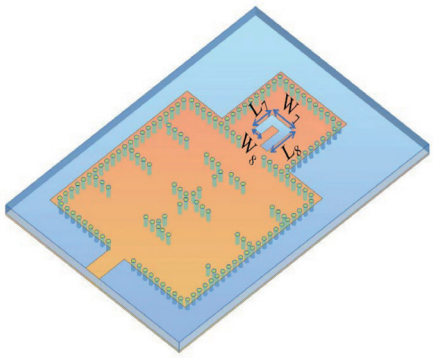

Fig. 4. (Color online) Geometry of SIW filtering antenna with dimensions $L_7 = 2.6$, $W_7 = 3$, $L_8 = 3.7$, and $W_8 = 1$ (all values in mm); others are the same as those of the design in Fig. 2.

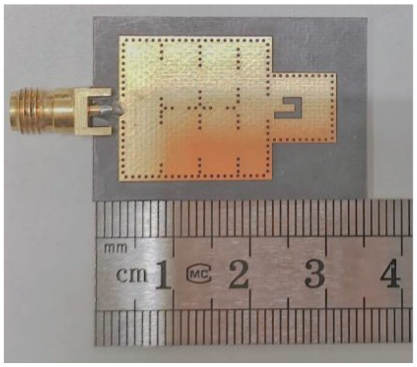

Fig. 5. (Color online) Fabrication prototype of proposed filtering antenna.

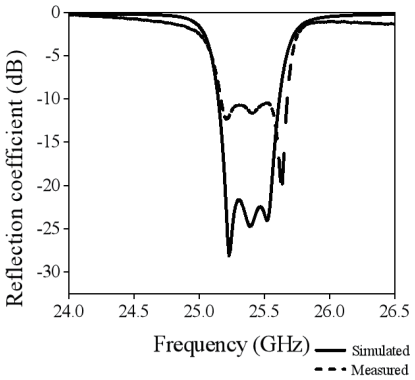

Fig. 6. Simulated and measured reflection coefficients.

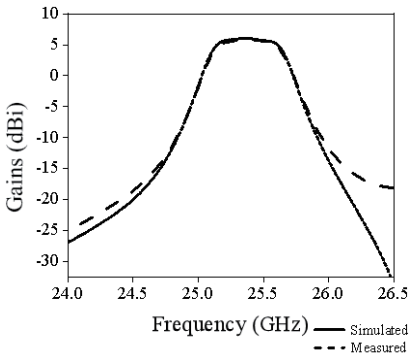

Fig. 7. Simulated and measured gains.

the simulation and measurement results may be related to manufacturing errors and changes in the dielectric constant and loss of the substrate. The designed antenna has a flat antenna gain of about 5.9 dBi, and the antenna gain fluctuation within the passband is less than ± 0.5 dBi.

Figure 8 shows the normalized simulation and measurement results of radiation patterns on two orthogonal planes at a frequency of 25.4 GHz. The measurement results are slightly different from the simulation results, which may be due to the reflection effect of the connectors and feeding cables during the measurement process.

The simulated and measured radiation efficiencies and standing wave ratios are shown in Figs. 9 and 10, respectively. In the passband of 25.2–25.7 GHz, the standing wave ratio is less than 1.6, and the measured standing wave ratio is about 0.4 higher than the simulated value. The measured radiation efficiency is about 87%, slightly lower than the simulated value. The difference between the simulation and measurement results can be attributed to transmission losses caused by manufacturing tolerances in the feeding network.

Table 2 shows the results of a comparison between the SIW millimeter-wave filtering antenna we proposed and some other reported SIW filtering antennas. In Ref. 7, a SIW 3D filtering antenna with high selectivity and low cross polarization, operating at a center frequency of 31.5 GHz with a FBW of 1.56%, is proposed. It exhibits a return loss greater than 11 dB and achieves a maximum measurement gain of 6.79 dBi, but uses a four-layer SIW structure. In Ref. 8, a compact and highly selective linearly polarized SIW filtering antenna that does not require additional filtering circuits is introduced. The antenna operates at a frequency of 24.6–29.6 GHz, has a fractional impedance bandwidth of 18.45% and an average gain of 5.7 dBi, and adopts a five-layer SIW structure. In Ref. 9, a dual-polarization SIW filtering antenna is described, which covers 23.2–29.5 GHz, has a FBW of 23.9% and an average gain of 4.5 dBi, and adopts a six-layer SIW structure. Jin *et al.* fabricated a 1 × 4 filtered patch antenna array with a peak gain of 11.1 dBi and a three-layer SIW structure in the 27.15–28.55 GHz frequency range.[20] Compared with the performance of the other filtering antennas mentioned above, the single-layer structure of the designed filtering antenna is simple and easy to integrate with other circuits, has low losses, and has great potential for application in the 5G era.

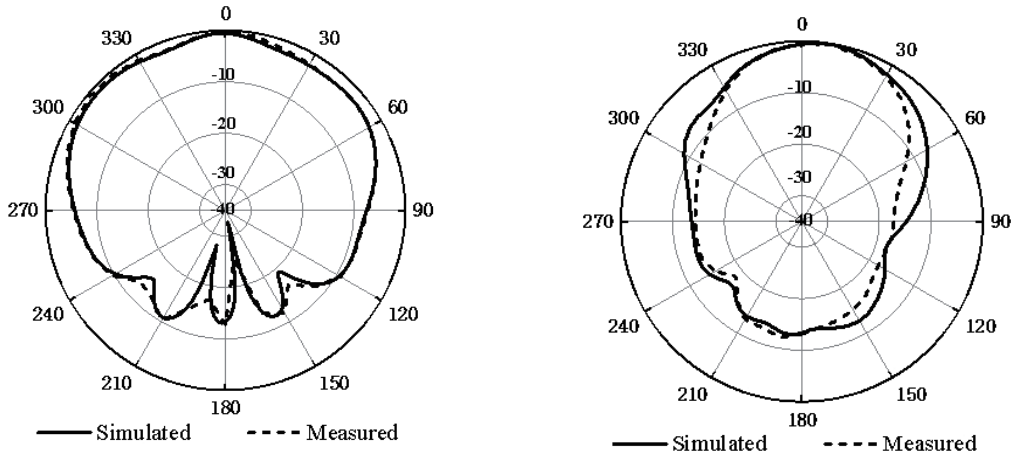

Fig. 8. Normalized filtering antenna radiation mode: (a) E-plane and (b) H-plane simulated and measured at 25.4 GHz.

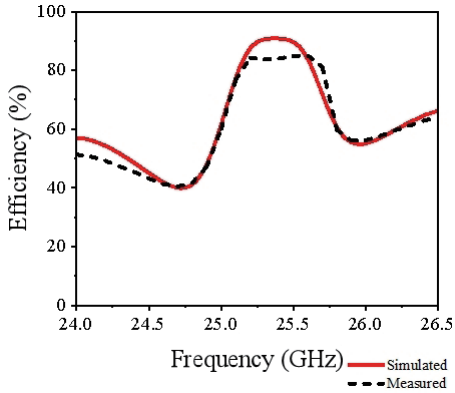

Fig. 9. (Color online) Simulated and measured radiation efficiencies.

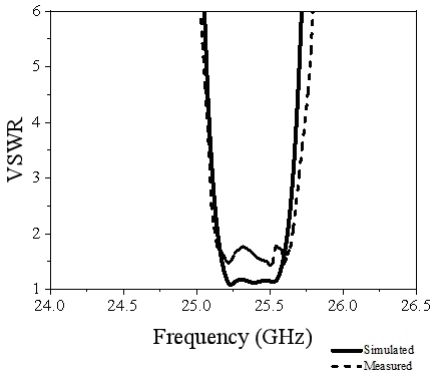

Fig. 10. Simulated and measured standing wave ratios.

Table 2
Results of comparison with other works.

Ref.	Antenna type	Imp.BW (−10 dB) (%)	Gain (dBi)	Polarization	Size (λ_0^3)	Layer
7	Single element	1.56%	6.79	Single	0.92 × 1 × 0.1	4
8	Single element	18.45%	5.7	Single	0.63 × 0.38 × 0.13	5
9	Single element	23.9%	4.5	Dual	0.35 × 0.49 × 0.2	6
20	1 × 4 subarray	5.03%	11.1	Single	3.08 × 2.52 × 0.2	3
This work	Single element	2%	5.9	Single	2.7 × 1.6 × 0.07	1

4. Conclusions

In this article, we proposed a millimeter-wave filtering antenna with a single-layer SIW structure based on a PCB process. The bandpass characteristics are formed by coupling the SIW cavities, and the Γ-shaped slot is etched in the last cavity of SIW to produce the radiation

characteristics. The measured operating frequency range of the SIW filtering antenna is 25.2–25.7 GHz, with a flat antenna gain of 5.9 dBi in the passband. The measurement results are in good agreement with the simulation results. The filtering antenna has a simple structure, low loss, and high out-of-band suppression level, and it is easy to integrate with other circuits. This filtering antenna has broad application prospects in the 5G-FR2 millimeter-wave band, electromagnetic sensor systems, and other fields.

Acknowledgments

This work was supported by the Fujian Natural Science Foundation Project (2022J01823) and the Leading Project of Fujian Science and Technology Plan (2023H0015).

References

1 T. S. Rappaport, S. Sun, R. Mayzus, H. Zhao, Y. Azar, K. Wang, G. N. Wong, J. K. Schulz, M. Samimi, and F. Gutierrez: IEEE Access **1** (2013) 335. https://doi.org/10.1109/ACCESS.2013.2260813
2 S. J. Yang, Y. M. Pan, L.-Y. Shi, and X. Y. Zhang: IEEE Trans. Antennas Propag. **68** (2020) 5114. https://doi.org/10.1109/TAP.2020.2975534
3 J. Deng, S. Hou, L. Zhao, and L. Guo: IEEE Antennas Wirel. Propag. Lett. **16** (2017) 2734. https://doi.org/10.1109/LAWP.2017.2743258
4 M.-C. Tang, T. Shi, and R. Ziolkowski: IEEE Trans. Antennas Propag. **64** (2016) 61. https://doi.org/10.1109/TAP.2015.2503732
5 M. Fakharian, P. Rezaei, A. Orouji, and M. Soltanpur: IEEE Antennas Wirel. Propag. Lett. **15** (2016) 1610. https://doi.org/10.1109/LAWP.2016.2518859
6 C.-K. Lin and S.-J. Chung: IEEE Antennas Wirel. Propag. Lett. **10** (2011) 381. https://doi.org/10.1109/LAWP.2011.2147750
7 B. Zhang and Q. Xue: IEEE Trans. Antennas Propag. **66** (2018) 4320. https://doi.org/10.1109/TAP.2018.2839968
8 T. Le Nadan, J. P. Coupez, S. Toutain, and C. Person: Proc. 1998 28th European Microwave Conf. (IEEE, 1998) 672−677. https://doi.org/10.1109/EUMA.1998.338067
9 J. Zuo, X. Chen, G. Han, L. Li, and W. Zhang: IEEE Antennas Wirel. Propag. Lett. **8** (2009) 141. https://doi.org/10.1109/LAWP.2009.2012732
10 K. Dhwaj, J. M. Kovitz, H. Z. Tian, J. J. Li, and I. Tatsuo: IEEE Antennas Wirel. Propag. Lett. 17 (2018) 833. https://doi.org/10.1109/LAWP.2018.2818058
11 Q. Wu, L. Zhu, and X. Zhang: IET Microwaves Antennas Propag. **11** (2017) 2241. https://doi.org/10.1049/iet-map.2017.0354
12 H. Chu, C. Jin, J.-X. Chen, and Y.-X. Guo: IEEE Trans. Antennas Propag. **63** (2015) 2375. https://doi.org/10.1109/TAP.2015.2411282
13 L. Fan, R. Lu, Y. Hu, and W. Hong: Proc. 2021 IEEE MTT-S Int. Wireless Symp. (IEEE, 2021) 1−3. https://doi.org/10.1109/IWS52775.2021.9499370
14 R. Lu, C. Yu, F. Wu, Z. Q. Yu, L. Y. Zhu, J. Y. Zhou, P. P. Yan, and W. Hong: IEEE Trans. Antennas Propag. **69** (2021) 5269. https://doi.org/10.1109/TAP.2021.3061110
15 K. Wu, D. Deslandes, and Y. Cassivi: Proc. 6th Int. Conf. Telecommunications in Modern Satellite, Cable and Broadcasting Service (IEEE, 2003) P-III. https://doi.org/10.1109/TELSKS.2003.1246173
16 D. Deslandes and K. Wu: IEEE Trans. Microwave Theory Techn. **54** (2006) 2516. https://doi.org/10.1109/TMTT.2006.875807
17 Y. Cassivi, L. Perregrini, P. Arcioni, M. Bressan, K. Wu, and G. Conciauro: IEEE Microwave Wireless Compon. Lett. **12** (2002) 333. https://doi.org/10.1109/LMWC.2002.803188
18 F. Xu and K. Wu: IEEE Trans. Microwave Theory Techn. **53** (2005) 66. https://doi.org/10.1109/TMTT.2004.839303
19 J.-S. Hong: Microstrip Filter for RF/Microwave Applications (John Wiley & Sons, 2011) 2nd ed., Chap. 3. https://doi.org/10.1002/0471221619
20 H. Jin, G. Q. Luo, W. Wang, W. Che, and K.-S. Chin: IEEE Access **7** (2019) 49804. https://doi.org/10.1109/ACCESS.2019.2909771

About the Authors

Haitao Xing was born in 1983 in Shandong, China. In 2010, he obtained a master's degree in communication and information engineering from Ningbo University. At present, his main research interests are in embedded systems, artificial intelligence, and IoT. (xht2005@jmu.edu.cn)

Jianmei Huang was born in 2002 in Fujian Province, China. She is currently pursuing her B.S. degree with the Department of Communication Engineering at Jimei University, Fujian Province, China. Her research interests are in mm-wave technology and antenna technology. (hjm@jmu.edu.cn)

Zhonghua Ma was born in Gansu, China, in 1973. He received his Ph.D. degree in microelectronics from Lanzhou University in 2018. His present research interests include antenna techniques, RF circuit design, RFID systems, and IoT. (mzhxm@jmu.edu.cn)